

Article

Economic Feasibility of a Renewable Integrated Hybrid Power Generation System for a Rural Village of Ladakh

Shilpa Sambhi ¹, Himanshu Sharma ^{1,*}, Vikas Bhadoria ², Pankaj Kumar ¹, Ravi Chaurasia ¹, Giraja Shankar Chaurasia ¹, Georgios Fotis ³, Vasiliki Vita ³, Lambros Ekonomou ^{3,*} and Christos Pavlatos ⁴

¹ Department of Electrical and Electronics Engineering, SRM Institute of Science and Technology, Delhi-NCR Campus, Ghaziabad 201204, Uttar Pradesh, India

² Department of Electrical and Electronics Engineering, ABES Engineering College, Ghaziabad 201009, Uttar Pradesh, India

³ Department of Electrical and Electronic Engineering Educators, School of Pedagogical and Technological Education, 14121 Athens, Greece

⁴ Hellenic Air Force Academy, Dekelia Air Base, Acharnes, 13671 Athens, Greece

* Correspondence: himanshuresearch58@gmail.com (H.S.); leekonomou@aspete.gr (L.E.)

Abstract: This paper mainly dealt with the technical and economic feasibility of an off-grid hybrid power generation system for a remote rural Turtuk village of Ladakh, located in the northern part of India. The study showed that the proposed configured renewable integrated hybrid system, using Hybrid Optimization of Multiple Energy Resources (HOMER) software, efficiently met the energy demand, exhibiting optimum performance with low investment. The proposed PV(115 kW)/Wind(1 kW)/Battery(164 strings of 6 V each)/DG(50 kW) hybrid system was a highly commendable, feasible solution preferred from a total of 133,156 available solutions resulting from HOMER simulations. The net present cost and energy cost of the proposed configuration were \$278,176 and \$0.29/kWh, respectively. The proposed hybrid configuration fulfilled local load, with 95.97% reduced dominant harmful carbon dioxide emission, as compared to the sole use of a diesel generator power supply system. The technical performance of the hybrid system was ensured, with advantages including the highest renewable penetration and least unmet load. Furthermore, the analysis exclusively evaluated the impact of the system's economic parameters (namely, its expected inflation rate, nominal discount rate, and project lifetime) on the net present cost and cost of energy of the system using a noble single fix duo vary approach.

Keywords: decentralized energy system; solar photovoltaic; net present cost; levelized cost of energy; renewable penetration; sensitivity analysis



Citation: Sambhi, S.; Sharma, H.; Bhadoria, V.; Kumar, P.; Chaurasia, R.; Chaurasia, G.S.; Fotis, G.; Vita, V.; Ekonomou, L.; Pavlatos, C. Economic Feasibility of a Renewable Integrated Hybrid Power Generation System for a Rural Village of Ladakh. *Energies* **2022**, *15*, 9126. <https://doi.org/10.3390/en15239126>

Academic Editor: Ignacio Hernando-Gil

Received: 31 October 2022

Accepted: 29 November 2022

Published: 1 December 2022

Publisher's Note: MDPI stays neutral with regard to jurisdictional claims in published maps and institutional affiliations.



Copyright: © 2022 by the authors. Licensee MDPI, Basel, Switzerland. This article is an open access article distributed under the terms and conditions of the Creative Commons Attribution (CC BY) license (<https://creativecommons.org/licenses/by/4.0/>).

1. Introduction

The traditional method of producing electricity uses a centralized power station which generates electricity in very large quantities. This electricity is then transmitted and distributed to load centers. Remote locations that are at a distance from centralized power stations are often deprived of electricity. Due to the various geographical challenges faced by these remote areas, their electricity supply network is not connected to the national grid. Such communities generate electrical energy using diesel generator-based power plants to fulfill their energy needs [1]. The emergence of smart cities, intelligent transport, and smart devices is a growing demand for electrical energy globally. This growing demand has created a challenge, namely to develop an economical and efficient system. In order to meet supply and demand needs, a robust system is required to provide an uninterrupted power supply by optimally utilizing energy resources to generate electricity. Another important aspect of such a system is the ability to conduct thorough transmission planning from time to time. This planning helps to identify the need for transmission line expansion to support increasing demand for electricity and improve system reliability [2,3].

The Government of India launched an initiative aimed at connecting remote areas with the national grid and took steps to produce electricity using locally available renewable energy sources [4]. India's total installed power generation capacity is approximately 393 GW as of this writing [5]. This includes approximately 38% (nearly 151 GW) of power generation through renewable energy sources using solar energy, wind energy, hydro energy, etc. Power generation through fossil fuels like coal, lignite, and gas accounts for nearly 58% (i.e., 253 GW) and approximately 0.1% (i.e., 0.51 GW) is generated through DG. Furthermore, India has aimed to reduce the deployment of fossil fuels to generate power; with this perspective, the country announced the goal of generating 175 GW of electricity from renewable energy sources by the end of 2022 [6]. This included 100 GW of electricity generation through solar energy, with the rest from wind energy, biomass and hydro power. By 2030, India intends to be generating 500 GW of power from renewable energy sources [7,8]. This target can only be achieved when all states of the country achieve their respective targets within the specified timelines. As per new analyses, India is lagging behind schedule on the production required to achieve its respective targets for 2022 and 2030, because several states are behind on achieving individual targets [9]. Though it is necessary for all state governments to have consistent policies and work on local issues, it is equally essential to perform technical and economic analyses on different parts of country to evaluate the feasibility of a suitable combination of HPG systems. In order to meet targets for the years 2022 and 2030, India needs to install 42 GW of renewable energy each year [9].

With the introduction of distributed energy resources (DERs) or decentralized electricity generation [10,11], there is a transition in electricity generation and transmission methods. DERs generate electricity on-site, i.e., near the load centers. Solar PV arrays, wind turbines, combined heat and power systems, flywheels, and battery systems are some of the currently growing DER technologies [12]. The greenhouse gas emissions can be reduced in DERs, which uses clean fuels like solar and wind energy to produce electricity. This initiative focuses on bringing down pollution levels. DERs can work independently from the utility grid and directly supply electricity to the load. As a result, most DERs are not connected to the utility grid [13]. For those DERs connected to the utility grid, bidirectional flow of electrical energy is possible. In other words, the excess electricity generated from DERs can be supplied to the grid. If the electricity demands at the load end increase, then DER can take supply from the grid.

Renewable energy-based DERs produce sustainable, cost-effective electrical energy. Various countries across the globe have started exploring ways of producing electricity from renewable sources of energy [14,15]. The estimated worldwide electricity generation through renewable sources in 2019 has reached 2351 GW [16]. Approximately 33% of overall electricity generation is through renewable energy sources. Considering the economics and weather conditions of remote regions, the focus has moved to generating from a renewable hybrid power generation (HPG) system instead of a diesel generator (DG)-based power plant [17]. The government has had to provide subsidies in fuel prices for diesel generators, which imposes an extra economic burden. When the net present cost and operational cost were compared, hybrid power plants proved to be more reliable and cost-effective than DG-based power plants [18]. A desirable improvement in terms of cost, pollutant emission, and reliability can be achieved by combining different renewable energy sources like solar and wind to form an HPG system [19,20]. As renewable energy sources are available locally, many countries are designing policies to adapt them to generate clean energy [21,22]. Before commissioning, a planning analysis should be conducted for an off-grid HPG system, including technical and economic analyses, to understand the feasibility of the system [23,24]. The economic analysis of an HPG system can be done based on two policies: pricing based on time of use and wholesale government policy [25]. The government has also worked on a policy of gross metering, in which energy internet supports the bidirectional flow of electrical energy between the HPG system and main grid [26].

Although the electricity network has expanded significantly, residential communities in isolated areas still suffer power outages. Even if such communities are coupled to the main grid, they suffer from poor power quality and frequent blackouts. In some cases, connecting the community with the main grid may not be economically feasible due to high capital investment for installing the transmission and distribution network [27]. Though DG-based power plants have a low initial investment, the operating costs are high, and their efficiency is low [28]. It is also worthwhile to note that the reliability of standalone power plants based on solar and wind energy cannot be ascertained because of intermittent weather conditions [29,30]. Thus, the electricity demands of isolated regions could be fulfilled through an off-grid HPG system. Renewable energy sources like solar energy, wind energy, biomass, and bio-fuels compensate each other when sparsely available for electricity generation [31,32].

The amount of greenhouse gases, especially carbon, emitted by off-grid, DG-based power plants are substantial [33]. As such, various studies have been conducted to find suitable solutions for the production of clean energy using renewable resources and the reduction of greenhouse gases [34]. In order to create a sustainable energy ecosystem, the governments of many countries have begun to show interest in electricity generation through renewable resources [35]. This has encouraged people to invest in installation of solar plants in residences, which will have a positive impact on the environment. Middle Eastern countries face extreme temperatures with little rainfall, so these countries have begun adopting power generation through renewable resources [36]. This could help such countries lessen their contributions to global warming. Reinforcement learning was applied to find an optimal configuration for HPG systems [37]. This approach was based on proximal policy optimization, achieving reductions in greenhouse gases by approximately 28.5% upon adopting HPG systems. Additionally, a 300 MW coal-based power plant was integrated with a solar plant [38]. The aim was to reduce the emission of pollution by reducing the consumption of coal for power generation. An optimized solution was developed for an HPG system based on three policies on emission of carbon: carbon tax, carbon cap-and-trade, and carbon offset [39]. The emission of greenhouse gases was significantly reduced.

Based on the above analyses, the following facts can be considered regarding the commissioning of an HPG system at the proposed location:

- With ever-increasing demand for electricity due to the expansion of smart cities, electricity generation can be increased through the use of renewable energy sources available locally at the considered site.
- Remote areas could produce electricity by commissioning DG-based power plants through an off-grid method. However, such power plants result in high amounts of pollutive elements in the atmosphere.
- The Indian government has undertaken many initiatives to motivate electricity generation through renewable sources of energy.
- The concept of DERs show promise as a way to produce electricity at a reduced energy cost, as they consist of renewable sources of electricity generation (excluding DGs).
- An HPG system may be designed according to the desired location's weather conditions. Locally available fuel sources like biomass may also be considered to reduce diesel usage. DG can be part of the HPG system as a captive source of power generation if renewable sources fail to generate electricity.
- Much of the work has been done to promote installation of an HPG system to reduce pollution levels caused by electricity generation through coal-based power plants.

In this article, the technical and economic analysis was undertaken for a region located in south-central Asia in the union territory of Ladakh, situated in India. A remotely located village in Ladakh named Turtuk was selected for technical and economic assessment. This village is located at latitude 34°17.98" N and longitude 78°17.59" E, as shown in Figure 1. This region experiences both arctic and desert climates, and so it is often known as a cold desert. The temperature of the selected region varies widely during the daytime, and the

seasonal variation of temperature ranges between $-40\text{ }^{\circ}\text{C}$ during winters to $35\text{ }^{\circ}\text{C}$ during summers. Because of high altitude and low humidity, the radiation level in Turtuk village is as high as $6\text{ to }7\text{ kWh/m}^2/\text{day}$ [40,41]. Annual rainfall/snowfall is approximately 10 cm. The air in this region is very dry, and relative humidity varies from 6% to 24%. Therefore, this region has more than 300 sunny days in a year. The average wind speed of this region ranges between 6 to 8 m/s [32,42].



Figure 1. Map showing Turtuk village in Ladakh, India.

The reliability and quick response of HOMER (Hybrid Optimization of Multiple Energy Resources) software (Pro 3.15) for estimating the optimal components of HPG systems makes it suitable for optimizing power sources [43]. This software was used to study the effects of different storage technologies while in operation in PV/Hydrokinetic/Battery/DG configuration. Here, upon comparing load flow control strategies with load tracking control, it was determined that there was variation in the minimum state of charge with respect to net cost [44]. A new dispatch strategy was formulated using HOMER and MATLAB link controller. It was concluded that variations in fuel price did not affect the proposed strategy, as compared to load flow and cycle charging strategies [45]. An optimization study was performed on PV/Wind/DG configuration using HOMER, with peak load demand profiles for residential and commercial sectors [46]. An on-grid solar-based power plant was analyzed to meet the electricity demand of a rural area in India using HOMER, to lower the cost of energy [47]. Different dispatch strategies were studied for a village in Uttarakhand, India for PV/WT/DG/Battery and PV/DG/Battery configurations. In this case, a PV/DG/Battery configuration was considered the optimal solution as it offered low cost of energy and lowered emissions [48].

In the current study, an analysis was done using Hybrid Optimization of Multiple Electric Renewables (HOMER) software. The obtained optimization results were analyzed by comparing net present cost (NPC), the levelized cost of energy (LCOE), and renewable fraction of each system. LCOE was calculated for the commercial life of the technology incorporated in HPG system. It calculated the annual cost of individual components by considering the discount rates, and determined NPC by considering the relative time value of money. This analysis resulted in the best combination of renewable resources as per the lowest LCOE. An HPG system can reduce diesel consumption—and hence, the emission of greenhouse gases. It can also help to optimally balance technology and financial metrics while designing a micro-grid.

This paper was organized into five different sections. Section 1 introduces the work. The methodology of the proposed work was provided in Section 2, including the load estimation of the selected site. The configuration of the HPG system was given in Section 3. Finally, the results and its discussions were provided in Section 4, followed by the conclusion of the work.

2. Methodology

The current study was primarily based on HOMER software, which requires meteorological data and estimated load of the location as an input to the system. The software retrieves data from the National Aeronautics and Space Administration (NASA). Therefore, analysis of the weather characteristics and load estimation is essential before the design of the hybrid system can be undertaken using locally available resources.

2.1. Weather Characteristics and Load Estimation of the Selected Site

The energy received on earth from the sun is electromagnetic radiation. Solar irradiance is the power received from the sun per unit area. Thus, the amount of solar irradiance received at a particular region is the daily average of horizontal solar radiation globally, including the beam radiation received directly from the sun and the diffused radiation in the atmosphere. The estimation of annual electrical energy production from wind turbines is taken from the wind speed data of a particular region. Figure 2 shows the average solar global horizontal irradiation (GHI) and the clearness index of Turtuk village. GHI is the solar irradiance received on the horizontal surface of the earth. It is the summation of direct normal irradiance (DNI), diffuse horizontal irradiance, and ground-reflected radiation [49]. These data showed that the selected region experienced an average GHI of $4.89 \text{ kWh/m}^2/\text{day}$. As shown in Figure 2, the maximum solar GHI was observed during June as $6.84 \text{ kWh/m}^2/\text{day}$. The weather remained clear during this month. The selected region experienced an average clearness index of 0.586, as shown in Figure 2. Thus, the region had a good clearness index, and the PV array system received the optimum amount of sunlight to generate electricity. The monthly average temperature data are provided in Figure 3, with the annual average at $-10 \text{ }^\circ\text{C}$. The summer season in Turtuk village begins in June, with an average temperature of $-1.2 \text{ }^\circ\text{C}$. Wind energy also contributes to electricity production at night when there is no solar energy. At the time of this study, this village suffered from power outages and received power from the main grid for only 4 to 6 h. This region also experienced a wind speed of 7.26 m/s average, with maximum wind speed occurring in December, as shown in Figure 4.

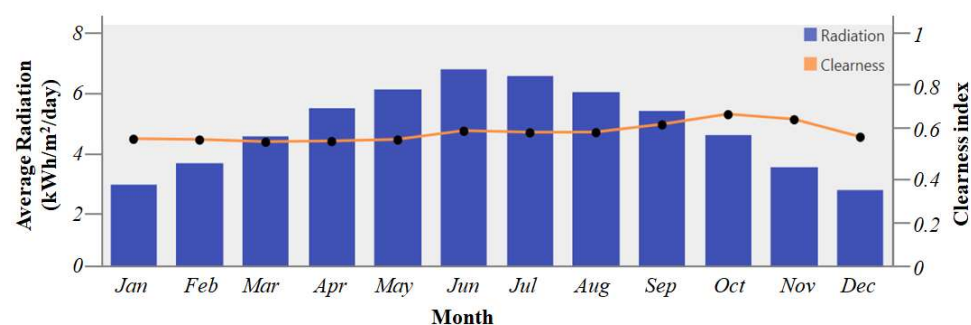


Figure 2. Solar irradiation and clearness index of the considered location.

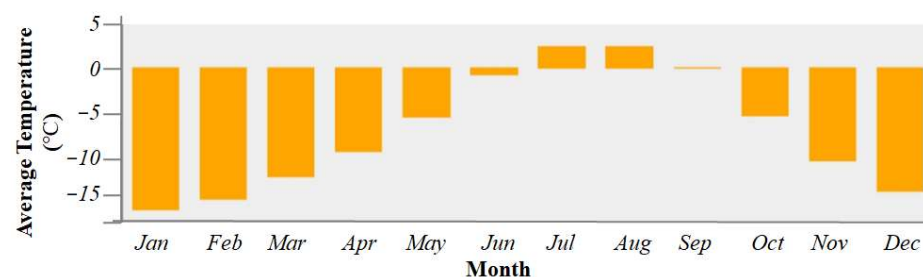


Figure 3. Monthly average temperature variation pattern of the location.

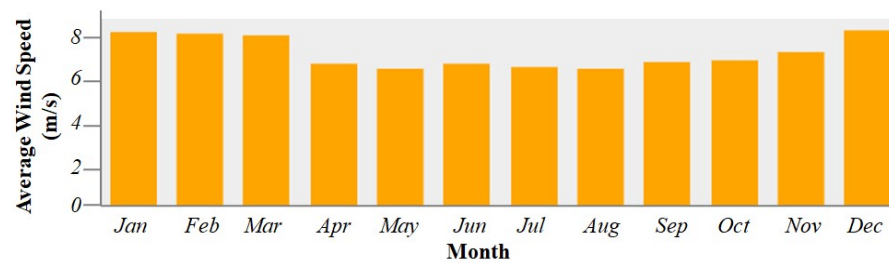


Figure 4. Monthly average wind speed variation of the location.

A comprehensive survey of the selected site was conducted to find the power consumption by load and estimate the load profile of a typical household. The village households consume power through five types of appliances. As shown in Table 1, the average load of compact fluorescent lamp (CFL) lighting per house was the highest among all the appliances in a given day. Radio consumed the lowest amount of electricity per day due to less usage. The total load of 300 households was taken as 199.5 kWh/day. The average consumption pattern for 24 h in a day of residential load is shown in Figure 5. It can be observed from Figure 5 that maximum electricity consumption occurred around the 19th hour of the day. The minimum consumption occurred between the first and fourth hour of the day. Likewise, the average monthly and yearly total electrical load served at the selected location is provided in Figures 6 and 7, respectively. It was observed that the electricity consumption in March and August was highest compared to other months.

Table 1. Estimated electrical load in the residential community of Turtuk village, Ladakh.

Load	Power (Watts)	Quantity	Usage Hours	Total Load (kWh)
TV	70	1	3	0.21
CFL light	25	1	9	0.225
LED light	10	2	10	0.2
Mobile charging point	3	1	6	0.018
Radio	2	1	6	0.012
Total load for one household				0.665 kWh/day
Total load for 300 households				199.5 kWh/day

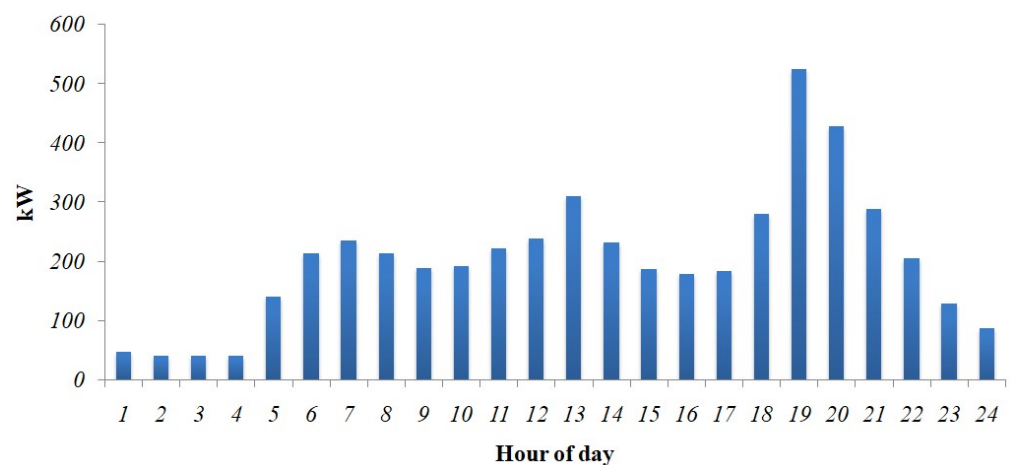


Figure 5. Daily residential load profile of the village.

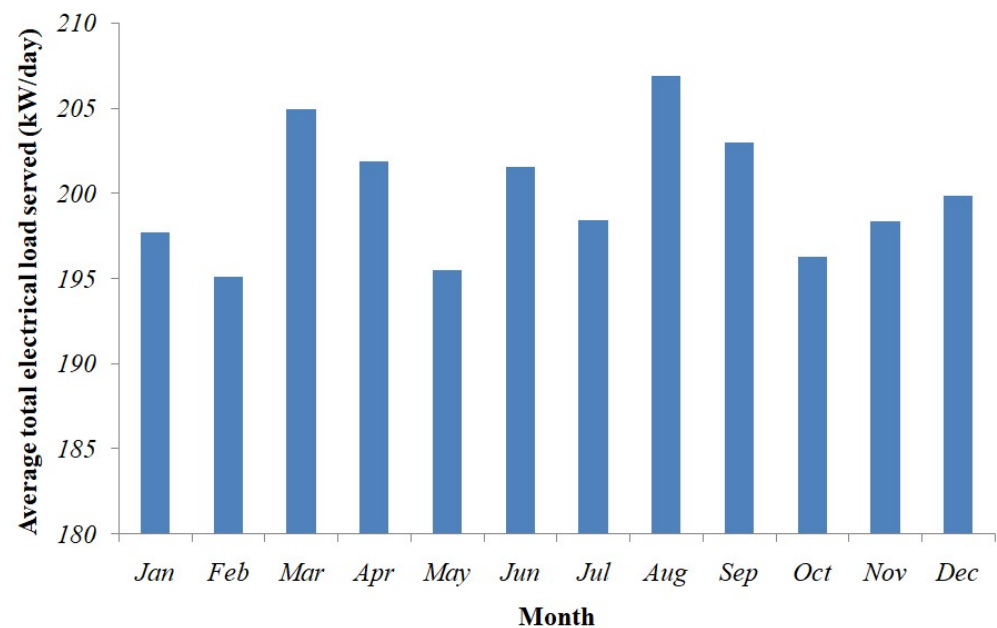


Figure 6. Monthly average load served at the village.

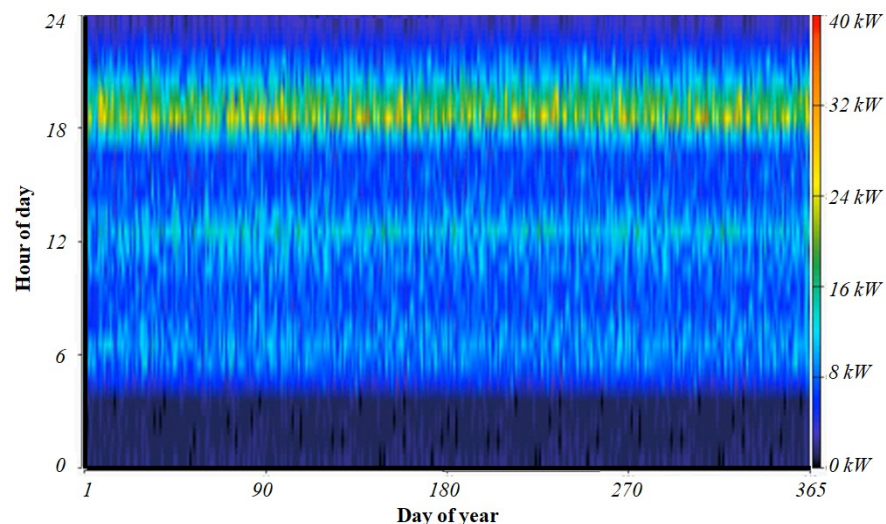


Figure 7. Yearly average total electrical load served at the village.

2.2. Simulation Tool for Hybrid Power Plant—HOMER Software

Various optimization approaches are available for conducting technical and economic analyses of hybrid power plants. They can be broadly classified into deterministic, stochastic, and hybrid approaches [50]. The deterministic approach, which includes linear programming, may not converge to a global solution because of the local optima entrapment problem. This problem of local optima entrapment can be resolved by a stochastic approach like genetic algorithm-based particle swarm optimization and iHOGA [51]. Such methods are computationally expensive and require significant memory space to store results. Hybrid approaches, such as simulated annealing-harmony search and simulated annealing-chaotic search techniques solve complicated real-world problems. HOMER uses grid search algorithms to simulate all feasible solutions, which is a hybrid approach.

Different software programs are available for finding the optimal solution [52]. General algebraic modeling systems can perform analyses for electrical and combined heat and power (CHP) systems to study and plan for hybrid power systems, as per government policy. Hybrid2, RAPSIm, and HYBRIDS are very user friendly and easy to utilize computer software programs to assist with long-term forecasts of hybrid power energy system

performance, but these do not provide economic analyses [51]. Technical and economic analyses of hybrid power systems can be compared with conventional power systems using RETScreen 8.0 software.

In this article, the chosen optimization tool for simulating hybrid power plants was the Hybrid Optimization of Multiple Energy Resources (HOMER) software. This software can simulate several available technologies with varying costs and variations in the availability of renewable energy sources. It includes optimization and sensitivity analysis algorithms to ease decision-making [53]. The software conducts several simulations to evaluate optimized solutions that can balance demand and supply of electricity. It provides the technical and economic perspective of different renewable energy sources by evaluating the loads served by the projected technology. Figure 8 shows the step-by-step chart of HOMER software. The algorithm used by HOMER software is provided as Figure A1 in Appendix A.

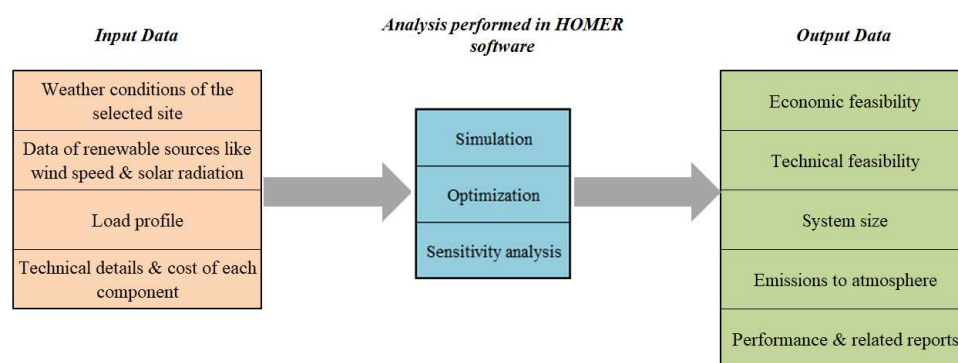


Figure 8. Flow chart of HOMER software tool.

3. Configuration of Hybrid Power Generation System

The components included in the HPG system included a solar photovoltaic (PV) array system, battery storage system (BSS), wind turbine, and DG. The PV array system, BSS, and wind turbine were connected to DC bus, while DG was connected to AC bus, as shown in Figure 9. The load connected to the HPG system required an AC power supply, while BSS required DC power to charge, so a converter was added to this hybrid system. The converter’s function was to optimize conversion from AC power to DC power and vice versa, depending on the direction of energy flow [54]. As power output from renewable resources depends on weather conditions, DG provided a necessary backup to the load in case of a shortfall from these resources. The proposed HPG system was expected to supply electricity to a residential community in Turtuk village, with an average and peak load of 200 kWh/day and 37.13 kW peak, respectively. These details and their related diagrams were acquired from HOMER software.

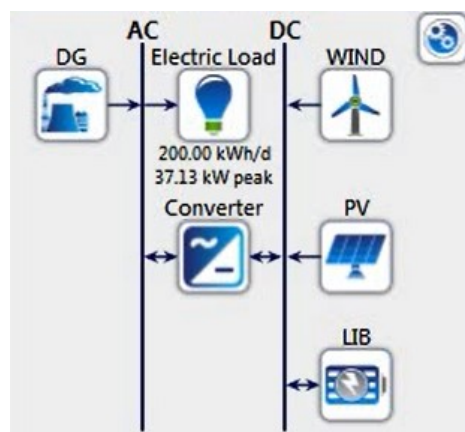


Figure 9. Schematic representation of hybrid power generation system.

3.1. PV Array

Turtuk is a high-altitude cold village in the rain shadows of the Himalayas with more than 300 days of sunshine and only 100 mm of precipitation annually [55]. The daily monthly average of radiation is 6–7 kWh/m²/day in summer and 3–4 kWh/m²/day, as presented graphically in Figure 2. Solar photovoltaic cells convert solar radiation into electrical power. The power produced by the PV array was computed through the specifications given by the manufacturer. The generic flat-plate PV was used to assess the proposed HPG system. The capital cost of solar panels was \$470 per kW and O&M cost was \$2.66 per year. The other technical specifications of this module are provided in Table 2. HOMER software has applied Equation (1) to calculate power output from the PV array [56]:

$$P_{\text{output}} = Y_{\text{PV}} f_{\text{PV}} \left(\frac{G_{\text{T}}}{G_{\text{T,STC}}} \right) [1 + \alpha_{\text{P}} (T_{\text{c}} - T_{\text{c,STC}})] \quad (1)$$

where Y_{PV} (kW) is the output power from PV array at standard test conditions (STC), f_{PV} (%) is the derating factor of PV array, G_{T} (kW/m²) is the solar radiation (which is incident on PV array), $G_{\text{T,STC}}$ (1 kW/m²) is the incident radiation from sun at STC, α_{P} (% per °C) is the power temperature coefficient, T_{c} (°C) is the temperature of PV cell in the current time step, $T_{\text{c,STC}}$ is temperature of PV cell under STC (25 °C). In case the effect of temperature on the PV array was not considered, HOMER assumed α_{P} to be zero, and Equation (1) was simplified, as presented in Equation (2) [57].

$$P_{\text{PV}} = Y_{\text{PV}} f_{\text{PV}} \left(\frac{G_{\text{T}}}{G_{\text{T,STC}}} \right) \quad (2)$$

Table 2. Technical specifications of the PV module.

Description	Value
Type of panel	Flat plate
Rated capacity (kW _p)	1
Capital cost (\$/kW)	470
Replacement cost (\$/kW)	470
O&M cost (\$/year)	2.66
Lifetime (years)	25
Derating factor (% assumed)	80

3.2. Wind Turbine

The considered location experienced an average wind speed of 7.26 m/s over the entire year. This became another renewable energy resource to generate electrical energy. The wind speed of a particular region is responsible for the amount of power produced by the wind turbine. HOMER calculates wind turbine output using the following three steps—(i) the wind speed is calculated at a particular hub height of wind turbine, (ii) the amount of power produced by a wind turbine at the wind speed, calculated in step (i), at standard air density, and (iii) finally, this output power value is attained for actual density of air. HOMER used Equation (3) to calculate output power from wind turbines [58].

$$P_{\text{WTG}} = \left(\frac{\rho}{\rho_0} \right) P_{\text{WTG,STP}} \quad (3)$$

where P_{WTG} (kW) is output power from wind turbine, $P_{\text{WTG,STP}}$ (kW) is output power from wind turbine at standard temperature and pressure (STP), ρ (kg/m³) is the actual density of air, ρ_0 is density of air at STP (1.225 kg/m³). It is essential to be familiar with the frequency distribution of wind in the selected site, which aids calculation of the amount of power

generated by the wind turbine. In other words, the power generated by a wind turbine depends on the wind speed at hub height. Wind power is calculated using Equation (4). In this equation, $v(z)$ represents the average wind speed at a new level, z , $v(z_a)$ is the average wind speed at anemometer level z_a , and α is the power index [59]. The power curve of the wind turbine is presented in Figure 10, which shows the amount of power produced at different wind speeds. The power generated by a wind turbine depends on the new hub-height wind speed at standard environmental conditions.

$$\frac{v(z)}{v(z_a)} = \left(\frac{z}{z_a}\right)^\alpha \quad (4)$$

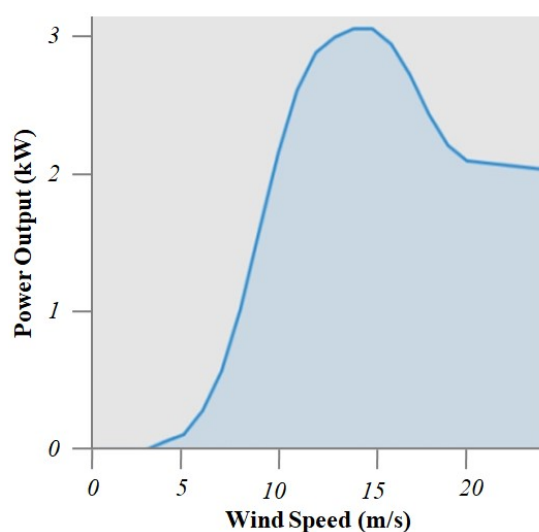


Figure 10. The power curve of the wind turbine.

To assess the proposed HPG system at the location, a generic 1 kW wind turbine was considered. The capital cost of the wind turbine is \$5000 per kW and O&M cost is \$50 per year. The other technical specifications of this module are given in Table 3. As shown in Figure 10, the power curve of the wind turbine was drawn based on three parameters: (1) the cut-in speed of the selected wind turbine was approximately 4 m/s, which meant that the turbine generated power up until this point; (2) the rated speed of this wind turbine was approximately 14 m/s, and generated 3 kW at this speed; and (3) the cutoff speed was approximately 15 m/s. If the cutoff speed were to be exceeded, the wind turbine would feather its blades, and its rotor would stop working. Hence, it would not generate power after exceeding the cut-off point. In this case, the turbine monitored wind speed. The turbine was designed to resume operation once the speed fell below the cutoff point for a specified duration [58].

Table 3. Technical specifications of the wind turbine.

Description	Value
Manufacturer	Generic
Rated capacity (kW)	1
Hub height (m)	17
Capital cost (\$/kW)	5000
Replacement cost (\$/kW)	5000
O&M cost (\$/year)	50
Lifetime (years)	25

3.3. Battery Storage System

The excess energy generated from renewable energy sources can be stored in devices like batteries. Whenever power from the grid is not available, the load can be powered using this stored energy. Moreover, it is beneficial to increase the renewable penetration in the HPG system in order to permit turning off the DG during the daytime. Another benefit is that the BSS stores the excess power produced and prevent edit from going to waste. This ensures a consistent power supply in case of a shortfall from renewable energy sources. As BSS forms an essential component of the HPG system, monitoring the battery state-of-charge (SOC) becomes vital. It protects the battery from overcharge and improves its life. In other words, the SOC of a battery is defined as the ratio of its current capacity ($Q(t)$) to the nominal capacity (Q_n) (refer Equation (5)) [59].

$$\text{SOC}(t) = \frac{Q(t)}{Q_n} \quad (5)$$

The batteries become useless either from use in the system or from aging. In other words, the lifetime of batteries may be limited by two independent factors: lifetime productivity and float life of storage. HOMER calculated the life of the battery bank using Equation (6) [60].

$$R_{\text{batt}} = \begin{cases} \frac{N_{\text{batt}} Q_{\text{lifetime}}}{Q_{\text{thrpt}}} & \text{If limited by productivity} \\ R_{\text{batt},f} & \text{If limited by lifetime} \\ \text{MIN} \left(\frac{N_{\text{batt}} Q_{\text{lifetime}}}{Q_{\text{thrpt}}}, R_{\text{batt},f} \right) & \text{If limited by productivity and lifetime} \end{cases} \quad (6)$$

where, R_{batt} (year) is life of storage bank, N_{batt} is number of batteries used in storage bank, Q_{lifetime} (kWh) is lifetime productivity of a single battery, Q_{thrpt} (kWh/year) is annual storage productivity, $R_{\text{batt},f}$ (year) is storage float life. To assess the proposed HPG system, generic 1 kWh Li-Ion batteries were used. The capital cost of the module was \$500 per kWh and estimated throughput was 3000 kWh. The technical specifications of this battery are given in Table 4.

Table 4. Technical specifications of the battery.

Description	Value
Nominal voltage (V)	6
Nominal capacity (kWh)	1
Maximum charge current (A)	167
Estimated throughput (kWh)	3000
Capital cost (\$/kWh)	500
Replacement cost (\$/kWh)	455
Lifetime (years)	10

3.4. Diesel Generator

DG provides an optimal solution for captive power generation due to diesel engines' high efficiency and low initial investment compared to steam turbines. Mainly, generators of sizes ranging between 4 to 15 MW are used in micro-grids. Low-speed diesel generators are more cost-effective than high-speed diesel generators [61]. The fuel consumption of the diesel generator per hour varies with load demand. HOMER software plotted a fuel curve, as shown in Figure 11, representing the fuel consumption based on the generator's output power. HOMER software uses the linear least-squares method to fit a line to the data points. The intercept on the y -axis represents "no-load fuel consumption". In other words, this intercept represents the amount of fuel consumption when the generator is idling (producing no electricity). The slope of this fuel curve is known as "marginal fuel

consumption". HOMER used Equation (7) to calculate the fuel consumed by the generator based on the electrical power generated [59].

$$F = F_0 Y_{\text{gen}} + F_1 P_{\text{gen}} \quad (7)$$

where F_0 (L/h/kW) is coefficient of intercept of fuel curve, F_1 (L/h/kW) is slope of fuel curve, Y_{gen} (kW) is the generator rated capacity, P_{gen} (kW) is generator power output. HOMER calculated the generator's efficiency at different points between zero and rated output and plotted the results as the efficiency curve, shown in Figure 12. For assessing the proposed HPG system, a generic small diesel generator was considered. The capital cost of this component was \$665 per kW and O&M cost was \$0.027 per hour. The price of fuel, accessed on 26 November 2021, was \$1.18 per litre [62]. The other technical specifications are provided in Table 5.

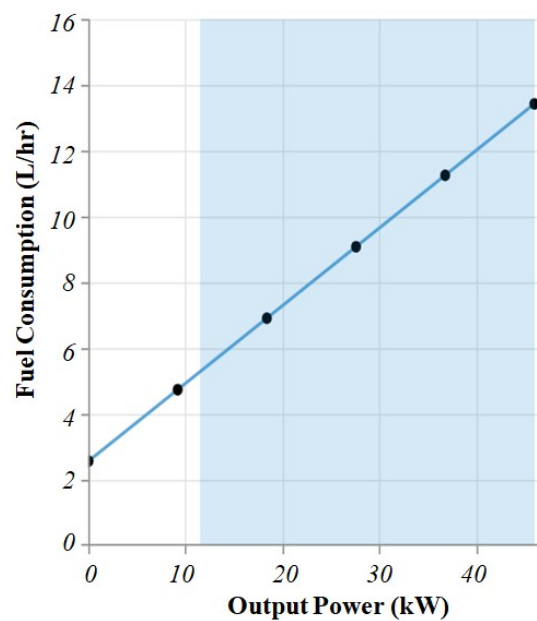


Figure 11. Fuel curve of the diesel generator.

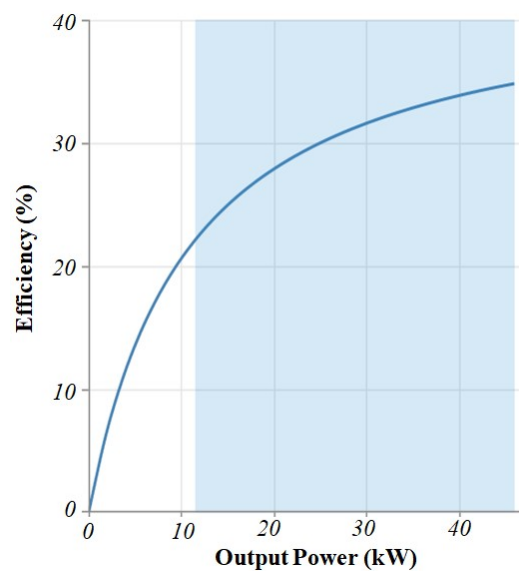


Figure 12. Efficiency characteristics of diesel generator.

Table 5. Technical specifications of diesel generator.

Description	Value
Fuel	Diesel
Capacity (kW)	1
Capital cost (\$/kW)	665
Replacement cost (\$/kW)	535
O&M cost (\$/hour)	0.027
Fuel price (\$/litre)	1.18
Lifetime (hours)	15,000

3.5. Converter

The proposed HPG system consisted of both AC and DC buses. A bidirectional converter was used to regulate the current flow direction during BSS charging and discharging. The size of this converter depended on the SOC level of the battery. The capacity of the converter was 1 kW. The capital cost of this converter was estimated to be \$195 per kW, with an O&M cost of \$4 per year, and the replacement cost was estimated to be \$195. It was rated for a lifetime of 15 years.

3.6. Economic Analysis

The feasibility of the simulated HPG system was assessed using LCOE. It was calculated as the ratio of the sum of the capital, operation and maintenance expenditure, and other related costs, estimated for the project's lifetime to the electrical energy generated in the entire lifetime of the hybrid power plant. A discount of 8% and an inflation rate of 2% were considered in the calculations. LCOE was calculated using Equation (8) [63].

$$\text{LCOE} = \frac{\sum_{t=1}^n \frac{I_t + M_t + F_t}{(1+r)^t}}{\sum_{t=1}^n \frac{E_t}{(1+r)^t}} \quad (8)$$

where I_t (\$) is the capital expenditure, M_t (\$) is expenditure for operation and maintenance, F_t (\$) is expenditure of fuel, E_t (kW) is the electrical energy generation, r (%) is rate of discount and n (years) is lifetime of the system. The obtained values of LCOE can be used to compare different technologies like wind, solar, generator, or combination, concerning life spans, capital cost, and ROI. In this article, the layout of the proposed HPG system was considered based on the optimal NPC. It was defined as the current value of the total cost minus the present value of total revenue over its life span [64]. Total costs included capital investment, cost for replacement, operation and maintenance (O&M) costs, fuel costs, penalties paid for emissions, and the costs of purchasing electricity from the grid. Total revenue included salvage cost and grid sales revenue. HOMER software calculated total NPC for all the system layouts during optimization. This value became the economic base for calculating the total annualized cost of the components and LCOE.

The salvage value is also an important economic parameter to assess the economic performance of a hybrid system. During NPC calculation, the remaining value of the components of the proposed HPG system, at the end of the project's life span, called the salvage value, was also considered. HOMER made two assumptions during calculation of salvage value: first, that (a) components depreciate linearly, meaning that the salvage value of components was directly related to their remaining life spans, and (b) that salvage value depends on the cost of replacement. HOMER calculated salvage value

using Equation (9) [59]. In the various cost calculations, HOMER applied an annual rate of interest because it presumed that all prices rose at the same rate.

$$S = C_{\text{rep}} \frac{R_{\text{rem}}}{R_{\text{comp}}} \quad (9)$$

where, C_{rep} (\$) is replacement cost of component, R_{rem} (years) is remaining life span of component (t) and R_{comp} (years) is life span of component (t).

3.7. Optimization Problem, Objective Function, Constraints

In the current study, the optimization problem was to analyze the HPG system and obtain minimum NPC, minimum COE, and minimum emission of pollutants in the atmosphere, along with maximum renewable resource fraction, for 24 h uninterrupted power supply. As such, the objective function of this problem was to minimize NPC and LCOE; in other words, Equation (8) was optimized to obtain the minimum value. The constraints considered in this analysis were: (1) derating factor of PV array was 80%, (2) hub height of wind turbine was 17 m, (3) for BSS, SOC ranged between 20 and 100%, and (4) minimum load ratio was 25% for DG. The lifetime of the HPG system was assumed to be 25 years.

4. Results and Discussions

The simulation was done considering a project lifetime of 25 years in HOMER software. The results obtained from the simulation assisted in choosing an optimal configuration for the HPG system. A total of 133,156 solutions were simulated by HOMER software, out of which nine optimized configurations of HPG system were obtained for attaining the minimum cost of energy, as presented in Table 6. The HOMER software performed simulations for all combinations, using PV array system, wind turbine, DG, and BSS. The PV-Wind-BSS-DG configuration attained the minimum cost of energy, considered the optimal low-cost solution with respect to the other solutions. In this study, the load-following (LF) control strategy was also considered. In this strategy, the generator operates only enough to meet the demand of the primary load. The charging of battery is done when renewable sources of energy like solar panels and wind turbines operate. In the LF control strategy, the generator can still produce more electricity to sell to the grid, if it has economic benefits. In simulations performed by HOMER, the program considered a shortfall occurring between the required operating capacity and the actual amount of operating capacity the system can provide. This figure is represented as capacity shortage constraint [64]. The sensitivity analysis was also conducted. These comparisons helped to determine the economic viability of the project. The average daily residential load for the considered location was predicted to be approximately 200 kWh/day. The average load was 8.33 kW/day, and the peak load was 37.13 kW. The daily consumption pattern of the residential load is shown in Figure 5.

Table 6. Optimized response from the HOMER software.

Architecture					Cost			
PV Array (kW)	Wind Turbine (kW)	Diesel Generator (kW)	Li-Ion Battery (kWh)	Converter (kW)	NPC (\$)	Cost of Energy (\$/kWh)	Operating Cost (\$/year)	Initial Capital (\$)
115	1	50	164	32	278,176	0.29	7542	180,672
369			219	42	384,750	0.40	7253	290,983
370	1		218	42	389,860	0.41	7275	295,818
		50	60	39	629,078	0.66	43,186	70,786
	1	50	58	41	634,618	0.67	43,275	75,176
253		50		21	874,726	0.92	55,580	156,220
216	1	50		21	880,339	0.93	56,969	143,870

Table 6. *Cont.*

Architecture			Cost			
	50		1,081,468	1.14	81,084	33,250
1	50	0	1,087,169	1.15	81,134	38,307
Total solutions simulated: 133,156						
Feasible solutions					98,110	
Infeasible solutions due to capacity shortage constraint					35,046	

4.1. *Technical and Economic Analysis*

The proposed configuration for the HPG system consisted of PV (115 kW)/Wind (1 kW)/BSS (164 strings of 6 V each)/DG (50 kW). It had LCOE, NPC, and operating costs of \$0.29 per kWh, \$278,176, and \$7542, respectively. The cost summary of the components for this configuration is indicated in Table 7. BSS made up 49.96% of the capital cost in this configuration, while the PV array system constituted 20.91%. The wind turbine comprised only 2.02% due to high capital and replacement cost. The DG made up 23.50% of the total cost, and the system converter was only 3.59% of the capital cost. The NPC and annualized cost of the above mentioned components are compared in Figure 13. NPC provide estimation of cash flow, showing the present value of installation and O&M over the lifetime of the component, while annualized cost differentiated the components as (1) low capital and high O&M and (2) high capital and low O&M costs. DG fell under the former category, while PV, wind turbine and BSS fell under the latter. In this layout of the HPG system, renewable energy sources constituted 22.94% of the total cost. In contrast, DG, BSS, and converter constituted 77.06% of the total cost.

Table 7. Component-wise cost summary of the low cost PV-Wind-BSS-DG hybrid configuration.

Component	Capital Cost (\$)	Replacement Cost (\$)	O&M Cost (\$/year)	Fuel Cost (\$)	Salvage Cost (\$)	Total Cost (\$)
Battery	82,000	65,922	0	0	−8937	138,984
Wind turbine	5000	0	646	0	0	5646
PV array	54,209	0	3966	0	0	58,175
Diesel Generator	33,250	0	6335	28,316	−2531	65,370
Converter	6212	2635	1647	0	−496	9999
System	180,671	68,557	12,595	28,316	−11,965	278,176

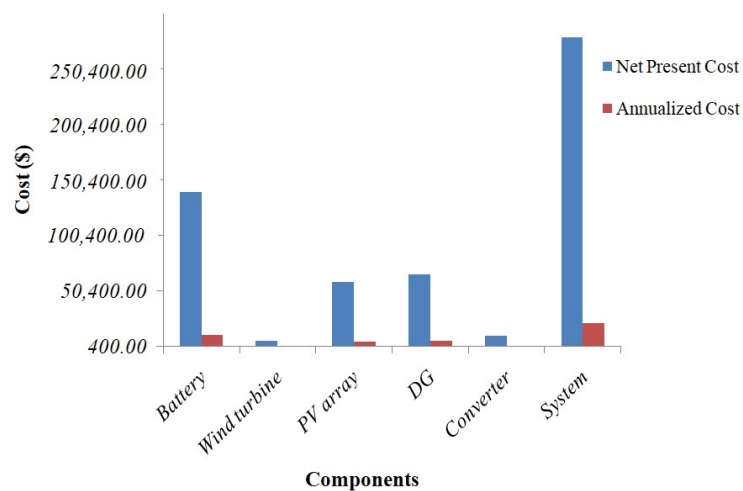


Figure 13. Component-wise cost summary for PV-Wind-BSS-DG configuration.

The simulation results from HOMER software showed that the PV-Wind-BSS-DG configuration could generate 184,689 kWh per year of electrical energy. This total electricity generation is the summation of 180,030 kWh per year from the PV array, 53.3 kWh per year from the wind turbine, and 4606 kWh per year from DG. In other words, the PV array produced 97.5%, wind turbine produced 0.0288%, and DG produced 2.49% of total electricity produced. Electricity generated from DG was the lowest because it was intended to only be operated when renewable sources failed to serve the load. Figures 14 and 15 present power output from PV array and wind turbine, respectively. Figure 16 indicates the electricity generated by DG. The monthly generation of electricity from the wind turbine, PV array, and DG is shown in Figure 17.

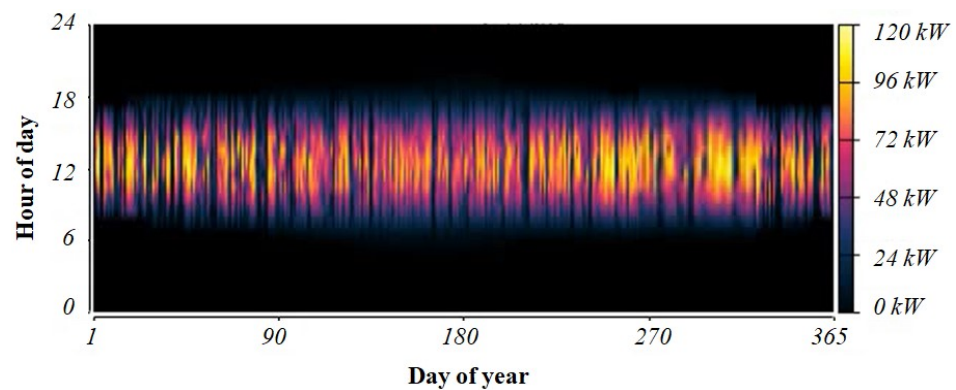


Figure 14. Yearly power output from PV array for PV-Wind-BSS-DG configuration.

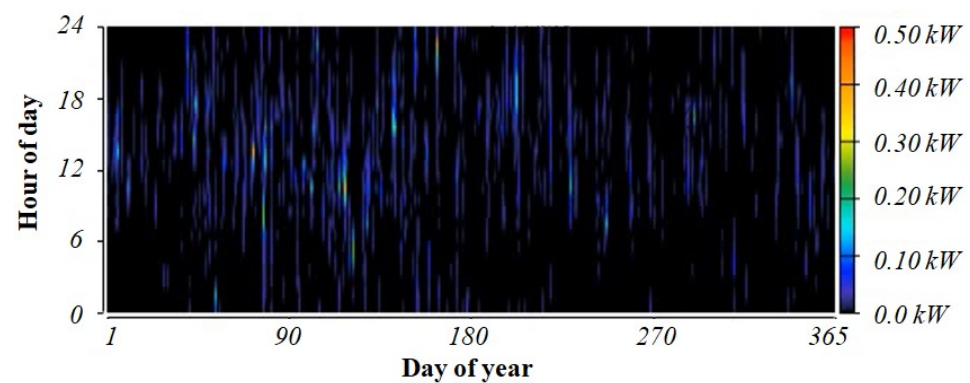


Figure 15. Yearly power output from wind turbine for PV-Wind-BSS-DG configuration.

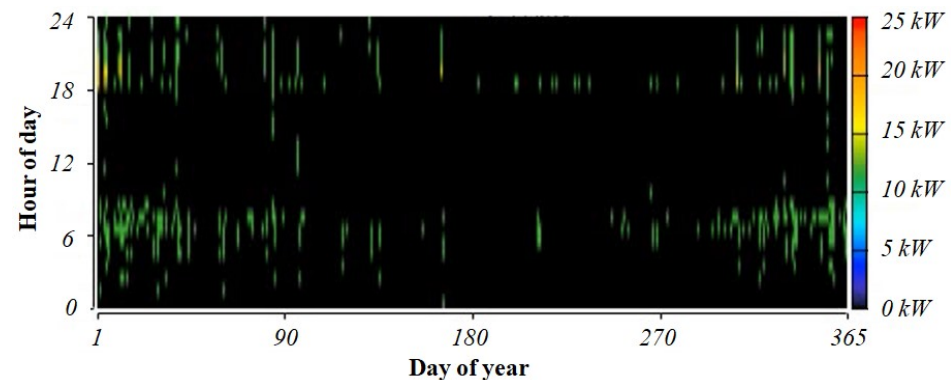


Figure 16. Yearly power output from diesel generator for PV-Wind-BSS-DG configuration.

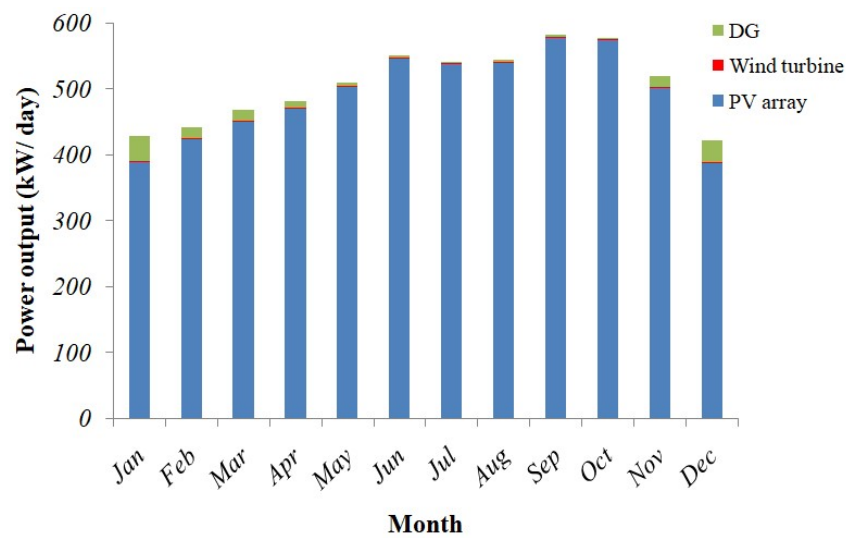


Figure 17. Monthly electricity production of PV-Wind-BSS-DG configuration.

In the simulation performed by HOMER software, the wind turbine was operated for 2413 h in a year. The electricity generated by the wind turbine was 53.3 kWh per year. The feasibility of the HPG system could be improved by optimally utilizing the weather conditions of the concerned location. DG served as a captive power generating source, available if renewable sources failed to generate sufficient electricity due to weather conditions or maintenance work.

It is imperative to determine the SOC level of a battery before it is put into operation. SOC refers to the amount of electric charge in a battery relative to its capacity. The SOC level of BSS for the proposed PV-Wind-BSS-DG configuration is shown in Figure 18. The batteries were charged between 54% to 72%, depending upon their usage and the weather conditions of Ladakh. The monthly profile of battery SOC is shown in Figure 19.

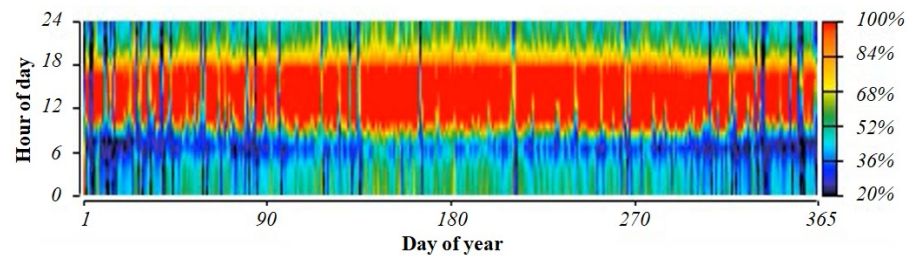


Figure 18. Yearly SOC profile of battery for PV-Wind-BSS-DG configuration.

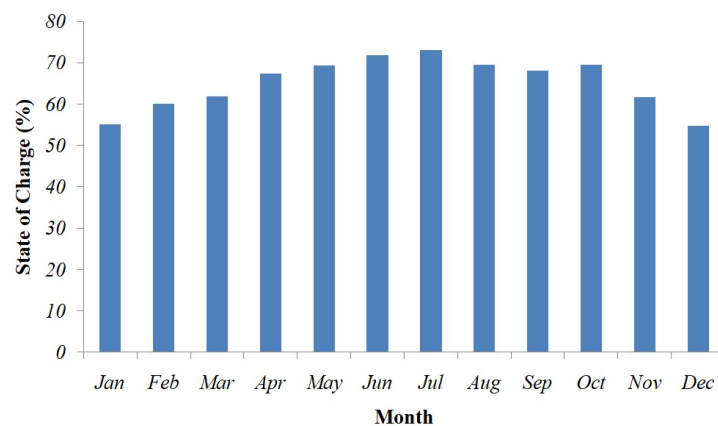


Figure 19. Monthly profile of SOC of battery for PV-Wind-BSS-DG configuration.

Figure 20 presents the 24-h time series curve for 1st January, to understand the relationship between supply and demand of electricity for the selected site. The individual contributions for electricity production from PV array, wind turbine, and DG are also presented. The following points were observed from the time-series curve:

- i. From hour 0 to the 7th hour, the entire load was served through the energy stored in BSS. PV array, wind turbine, and DG did not operate during this time.
- ii. From the 7th hour to the 17th hour, the load was served through electricity generated from the PV array and the energy stored in BSS. Arise in demand for electricity was experienced during this time. The wind turbine and DG were not operated during this time.
- iii. From the 17th hour to the 20th hour, as PV array could not generate electricity during the evening and night hours, the electricity demand was fulfilled through the operation of DG. The BSS supplied electricity until the 19th hour, and then it discharged. The SOC level of BSS remained at zero from 19th to 20th hours.
- iv. From the 20th hour to the 23rd hour, the demand for electricity decreased, but the load was served through DG only. During this time, the BSS also charged.

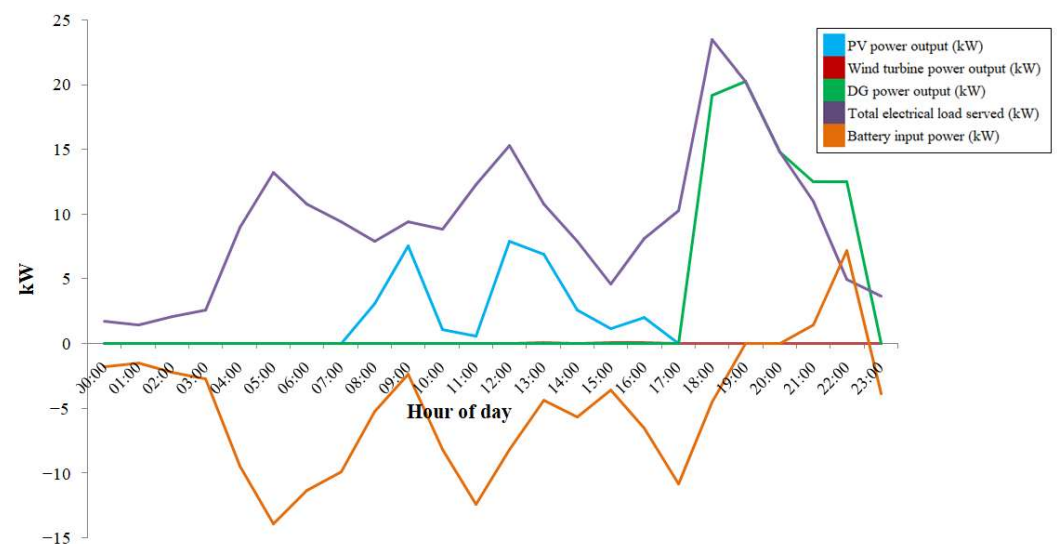


Figure 20. Time series power output trend of PV-Wind-BSS-DG configuration for 1st January.

4.2. Sensitivity Analysis

Sensitivity analysis is an economic model which gives an idea about the behavior of the variables under consideration, based on changes in other input variables. Another name of this model is what-if or simulation analysis. The NPC of a component is the current value. It includes the component's installation cost and operating cost; thus, NPC is also known as life-cycle cost. The cost of energy assessment is the average NPC of electricity generation from a power generating plant over its life span. This article considered three sensitivity variables: inflation, discount, and project lifetime. These variables were varied as (i) inflation rate: 2%, 4%, and 6%; (ii) discount rate: 6%, 8%, and 10%; and (iii) project lifetime: 20 years, 25 years and 30 years. However, the analyses used the noble single fix duo vary approach to investigate the impact of variation of these variables on system performance.

An optimization plot was plotted, keeping the project lifetime constant and varying cost of energy and renewable fractions, as presented in Figure 21, for the project lifetime of 25 years. Every point in the optimization plot was a feasible solution for that particular sensitivity case. As observed, most obtained solutions had a high renewable fraction with a low cost of energy.

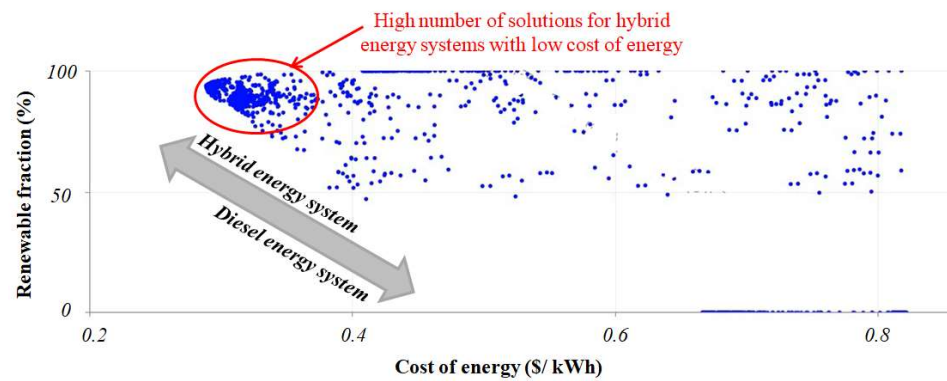


Figure 21. Optimization plot between renewable fraction and cost of energy with project lifetime of 25 years.

The cost of energy and NPC are affected by sensitivity variables. On the surface, NPC was plotted to have a clear overview, and the corresponding cost of energy was superimposed, as shown in Figure 22a–c. In this plot, the project lifetime was kept constant, and the inflation rate and discount rate were varied. This way, three surface plots were plotted for a project lifetime of 20 years, 25 years, and 30 years. It can be observed from these plots that as the inflation rate increased and the discount rate decreased, the cost of energy decreased.

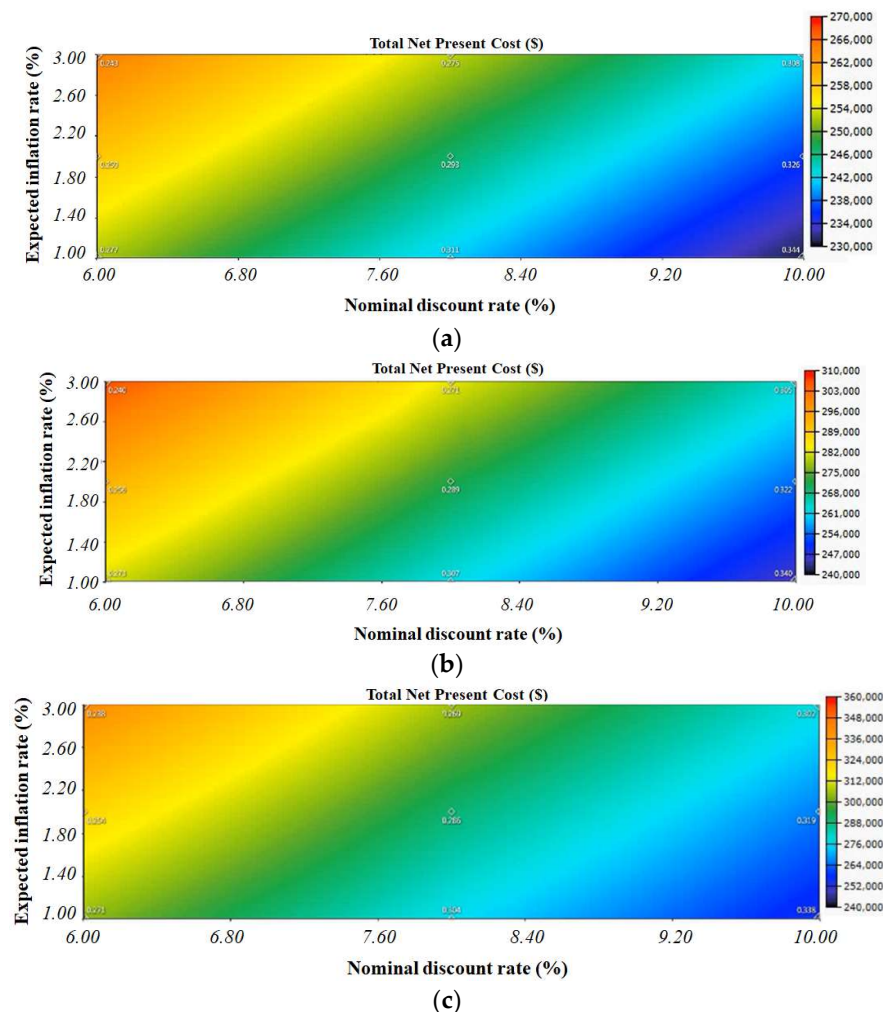


Figure 22. Variation in NPC as per inflation rate and discount rate with project lifetime of (a) 20 years, (b) 25 years, and (c) 30 years.

4.3. Comparison of Proposed HPG System with the Base Case

A DG-based power plant was taken as the base case, where HOMER software calculated a DG of 50 kW. A comparative study of PV-Wind-BSS-DG configuration was done with the base case, as shown in Table 8. The simulation performed by HOMER software for the base case calculated LCOE at \$1.14/kWh, operating cost at \$81,084/year, initial investment at \$33,250 and NPC at \$1,081,468. Apart from the high operating cost and NPC of the base case, the LCOE of this case was much higher than the PV-Wind-BSS-DG configuration. This was mainly because of the high rates of fuel (diesel) used to operate the generator. The rate of diesel fluctuates daily and can rise day by day. With the PV-Wind-BSS-DG configuration, the consumers could generate electricity with affordable low LCOE and low NPC. This could raise the economic development of this region.

Table 8. Comparative cost summary of the two compared hybrid systems.

Parameter	DG Only (Base Case)	PV-Wind-BSS-DG Configuration
Initial Capital (\$)	33,250	180,672
Operating cost (\$/year)	81,084	7542
Cost of energy (\$/kWh)	1.14	0.29
NPC (\$)	1,081,468	278,176

The world is already facing the challenge of reducing pollution. Different nations have focused on using renewable sources to generate electricity to aid in these efforts. Thus, the diesel-based case is not a feasible solution for implementation. The base case's carbon dioxide and other harmful gas emissions are 120,788 kg/year and 141,800.16 kg/year, respectively. On the other side, the proposed PV-Wind-BSS-DG configuration would emit only 4859 kg/year and 3804.14 kg/year of carbon dioxide and other harmful gasses emissions, respectively. This way, electricity generation through renewable sources of energy would help to reduce the emission of such polluting gases in the environment. A comparison of the emission of different pollutants from the proposed configuration and the base case is presented in Table 9.

Table 9. Comparison of emission of pollutants from different configurations.

Configuration	Total Fuel (Diesel) Consumed (Litre/Year)	Carbon Dioxide (kg/Year)	Carbon Monoxide (kg/Year)	Unburned Hydrocarbons (kg/Year)	Particulate Matter (kg/Year)	Sulfur Dioxide (kg/Year)	Nitrogen Oxides (kg/Year)
DG only (Base case)	46,140	120,788	754	33.2	4.52	296	709
PV-Wind-BSS-DG (Proposed)	1856	4859	30.3	1.34	0.182	11.9	28.5

The payback period refers to the time required to recover the investment cost of components. To calculate the payback period, the PV-Wind-BSS-DG configuration was compared with a reference system, also known as a conventional base case system. The DG-based power plant was considered the base case for comparison with the proposed configuration. The simulation estimated a 1.8-year payback period for PV-Wind-BSS-DG configuration. This payback period was deemed justifiable because Turtuk village is located in the Himalaya hilly region, and so the capital cost of installing a transmission and distribution system would be prohibitively high. In such a case, a renewable energy-based micro-grid could be an optimal solution to generate electricity in isolated rural regions.

A comprehensive study of the HPG system of different locations is provided in Table 10. Depending upon the weather conditions and locally available fuels, optimal configurations of the HPG system were analyzed. Puducherry, India, proposed an HPG system consisting

of PV-WT-Biogen, with NPC of \$16,365.95 and a cost of energy of \$0.19/kWh. An East African country proposed a Hydro-Solar-Battery configuration as an HPG system with \$41,210.80 NPC and \$0.056/kWh cost of energy. A district in Karnataka, India, proposed a PV-WT-BGG-BMG-FC-Battery to commission their HPG system. It had NPC and the cost of energy values of \$890,013 and \$0.214/kWh, respectively. Cities in the Gulf and a village in Iran have proposed a combination of PV-WT-Battery for HPG systems; NPC and the cost of energy are presented in Table 10. A configuration of PV-DG-Battery was submitted for a village in Ethiopia, with \$82,734 NPC and \$0.207/kWh cost of energy. PV-WT-DG-Battery was proposed for Ghana, an industrial city in Iran, and Tamil Nadu in India. Its respective NPC and cost of energy are provided in Table 10.

Table 10. Comparison of stand-alone hybrid systems at different locations.

Sr. No.	Location	Proposed Hybrid System	NPC (\$)	Cost of Energy (\$/kWh)	Reference
1	Korkadu, Union territory of Puducherry, India	PV-WT-Biogen	\$16,365.95	\$0.19	[17]
2	Rwanda, East African Country	Hydro-Solar-Battery	\$41,210.80	\$0.056	[65]
3	Chamarajanagar district, Karnataka, India	PV-WT-BGG-BMG-FC-Battery	\$890,013	\$0.214	[19]
4	Jask (near the Gulf of Oman)	PV-WT-Battery	\$44.1 M	\$0.219	[66]
	Genaveh (near the Persian Gulf)	PV-WT-Battery	\$46.9 M	\$0.233	
	Anzali (near the Caspian sea)	PV-WT-Battery	\$48.8 M	\$0.242	
5	Golbo II village, Ethiopia	PV-DG-Battery	\$82,734	\$0.207	[67]
6	Mankwadze, Ghana	PV-WT-DG-Battery	\$8,649,054	\$0.382	[42]
7	Rezwan village, Sudaklen, Iran	PV-WT-Battery	\$24,662	\$0.322	[68]
8	Leopard beach, Hongsibao, China	PV-WT-BGG-Battery	\$587,013	\$0.201	[69]
9	Industrial city II, Ardabil, Iran	PV-WT-DG-Battery	\$304,380	\$0.471	[70]
10	Fouay, Benin republic, Africa	PV-DG-Battery	\$555,492	\$0.207	[71]
11	Chikmagalur district, Karnataka, India	PV-Hydro-Battery	\$712,975	\$0.16	[72]
12	Singa village, Siang district, Arunachal Pradesh, India	WT-Hydro-DG-Battery	\$23,808	\$0.63	[73]
13	Tamilnadu, India	PV-WT-DG-Battery	\$199,850.80	\$0.2492	[74]
14	Ghaziabd, India	PV-BSS	\$639,981	\$0.34	[75]
15	Turtuk village, Ladakh, India	PV-Wind-BSS-DG	\$2,78,176	\$0.29	Present study

Legend: PV: Solar photovoltaic, WT: Wind turbine, Biogen: Bio generator, BGG: Biogas generator, BMG: Biomass generator, FC: Fuel cell, DG: Diesel generator.

A location in China proposed a PV-WT-BGG-Battery HPG system, with \$587,013 NPC and \$0.201/kWh cost of energy. An HPG system consisting of PV-DG-Battery was proposed for a location in Africa, with NPC and cost of energy values of \$555,492 and \$0.207/kWh, respectively. A PV-Hydro-Battery combination was proposed for Karnataka, India, and a WT-Hydro-DG-Battery combination was proposed for Arunachal Pradesh, India. A PV-WT-DG-Battery was proposed for a location in Tamilnadu, India. Its NPC and cost of energy values are provided in Table 10.

5. Conclusions and Future Prospects

The purpose of this work was to provide technical and economic perspectives on a proposed HPG system to generate electricity using renewable sources of energy in south-central Asia. The optimal solution and operation strategy for an HPG system for an isolated village in the Ladakh region were evaluated using HOMER software. The key parameters considered during the feasibility study were NPC, LCOE, and renewable fraction. According to the simulations performed by HOMER, the minimum cost of energy was obtained for a PV-Wind-BSS-DG configuration of the HPG system. It was chosen as

the optimal solution. DG served as a captive power generation system. The following conclusions were made regarding this work:

- i. The configuration of the proposed HPG system had a PV array of 115 kW, wind turbine of 1 kW, DG of 50 kW, BSS with 164 strings of 6V each, and a converter of 31.85 kW. The base case consisted of an isolated DG of 50 kW.
- ii. In the proposed PV-Wind-BSS-DG system, the total net present cost (NPC) of the system was reduced by 74.27%, from \$1,081,468 of diesel-based power generation system to \$278,176.
- iii. It was observed that the proposed system reduced the cost of energy from \$1.14 per kW in the diesel-based base case to \$0.29 per kW.
- iv. It was observed that the proposed system reduced the emission of pollutants up to 94.86%, from 168,724.72 kg/year to 8663.14 kg/year.
- v. A sensitivity analysis was performed, varying project lifetime, inflation rate, and discount rate. NPC and cost of energy were analyzed upon these sensitivity variables.

In future prospects, analyses could be further improved by considering government policies, subsidies, and tariffs. Governments, utility companies, and energy sector players are expected to make a calculated effort to implement transparent procedures to further develop the renewable sector.

Author Contributions: Resources, R.C., G.S.C., G.F., V.V., L.E. and C.P.; Supervision, H.S., V.B. and P.K.; Writing—original draft, S.S.; Writing—review and editing, H.S. and P.K. All authors have read and agreed to the published version of the manuscript.

Funding: This research received no external funding.

Data Availability Statement: The authors confirm that all data has been presented.

Conflicts of Interest: The authors declare no conflict of interest.

Appendix A

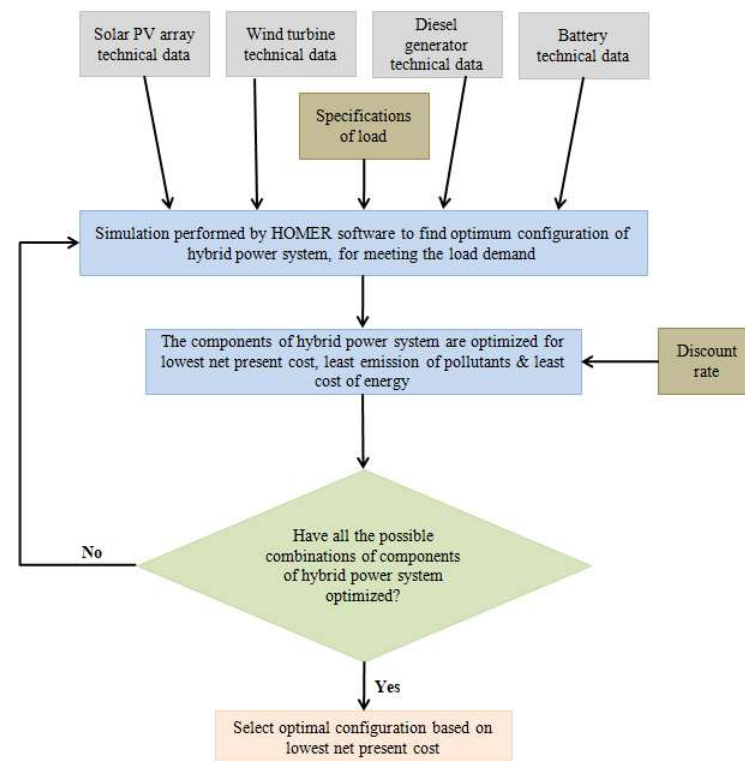


Figure A1. Flow chart of algorithm used by HOMER.

References

1. Ladakh's Remote Nubra, Zaskar Valleys to Get Connected to National Power Grid. Available online: <https://energy.economictimes.indiatimes.com/news/power/ladakhs-remote-nubra-zaskar-valleys-to-get-connected-to-national-power-grid/77737625> (accessed on 25 August 2020).
2. Ekonomou, L.; Fotis, G.; Vita, V.; Mladenov, V. Distributed Generation Islanding Effect on Distribution Networks and End User Loads Using the Master-Slave Islanding Method. *J. Power Energy Eng.* **2016**, *4*, 1–24. [CrossRef]
3. Sharma, H.; Pal, N.; Kumar, P.; Yadav, A. A control strategy of hybrid solar-wind energy generation system. *Arch. Electr. Eng.* **2017**, *66*, 241–251. [CrossRef]
4. Kumar, P.; Sharma, H.; Pal, N.; Sadhu, P.K. Comparative Assessment and Obstacles in the Advancement of Renewable Energy in India and China. *Probl. Ekorozw.* **2019**, *14*, 191–200.
5. Power Sector at a Glance ALL INDIA. Available online: <https://powermin.gov.in/en/content/power-sector-glance-all-india> (accessed on 10 February 2022).
6. India May Miss 2030 Renewable Energy Targets as UP, Punjab, Haryana Lag, Say Experts. Available online: <https://economictimes.indiatimes.com/industry/renewables/india-may-miss-2030-renewable-energy-targets-as-up-punjab-haryana-lag-say-experts/articleshow/90964081.cms> (accessed on 12 May 2022).
7. Homer Pro. Available online: https://www.homerenergy.com/products/pro/docs/latest/standard_test_conditions.html (accessed on 14 August 2020).
8. India to Have 450 GW Renewable Energy by 2030: President. Available online: <https://economictimes.indiatimes.com/small-biz/productline/power-generation/india-to-have-450-gw-renewable-energy-by-2030-president/articleshow/73804463.cms?from=mdr> (accessed on 8 June 2022).
9. Achieving 2022 Renewable Energy Targets Would Have Averted India's April Power Crisis. Available online: <https://economictimes.indiatimes.com/industry/renewables/achieving-2022-renewable-energy-targets-would-have-averted-indias-april-power-crisis/articleshow/91688224.cms> (accessed on 17 July 2022).
10. Eze, F.; Ogola, J.; Kivindu, R.; Egbo, M.; Obi, C. Technical and economic feasibility assessment of hybrid renewable energy system at Kenyan institutional building: A case study. *Sustain. Energy Technol. Assess.* **2022**, *51*, 101939. [CrossRef]
11. Kreishan, M.Z.; Fotis, G.; Vita, V.; Ekonomou, L. Distributed Generation Islanding Effect on Distribution Networks and End User Loads Using the Load Sharing Islanding Method. *Energies* **2016**, *9*, 956. [CrossRef]
12. Pepermans, G.; Driesen, J.; Haeseldonckx, D.; Belmans, R.; D'haeseleer, W. Distributed generation: Definition, benefits and issues. *Energy Policy* **2005**, *33*, 787–798. [CrossRef]
13. Kumar, P.; Pal, N.; Sharma, H. Performance analysis and evaluation of 10 kWp of solar photovoltaic array for remote islands of Andaman Nicobar. *Sustain. Energy Technol. Assess.* **2020**, *42*, 100889. [CrossRef]
14. Moustakas, K.; Loizidou, M.; Rehan, M.; Nizami, A.S. A review of recent developments in renewable and sustainable energy systems: Key challenges and future perspective. *Renew. Sustain. Energy Rev.* **2020**, *119*, 109418. [CrossRef]
15. Kumar, R.S.; Raghav, L.P.; Raju, D.K.; Singh, A.R. Customer-oriented energy demand management of grid-connected microgrids. *Int. J. Energy Res.* **2021**, *45*, 18695–18712. [CrossRef]
16. International Renewable Energy Agency. Available online: www.irena.org/newsroom/pressreleases (accessed on 10 August 2020).
17. Kumar, A.; Singh, A.R.; Deng, Y.; He, X.; Kumar, P.; Bansal, R.C. Integrated assessment of a sustainable microgrid for a remote village in hilly region. *Energy Convers. Manag.* **2019**, *180*, 442–472. [CrossRef]
18. Ghaithi, H.M.; Fotis, G.; Vita, V. Techno-Economic Assessment of Hybrid Energy off-Grid System—A Case Study for Masirah Island in Oman. *Int. J. Power Energy Res.* **2017**, *11*, 103–116. [CrossRef]
19. Wu, T.; Zhang, H.; Shang, L. Optimal sizing of a grid-connected hybrid renewable energy systems considering hydroelectric storage. *Energy Sources A Recovery Util. Environ. Eff.* **2020**, 1–17. [CrossRef]
20. Ren, Y.; Yao, X.; Liu, D.; Qiao, R.; Zhang, L.; Zhang, K.; Jin, K.; Li, H.; Ran, Y.; Li, F. Optimal design of hydro-wind-PV multi-energy complementary systems considering smooth power output. *Sustain. Energy Technol. Assess.* **2022**, *50*, 101832. [CrossRef]
21. Maqbool, U.; Tyagi, A.; Tyagi, V.V.; Kothari, R. Optimization of the renewable-energy-based micro-grid for rural electrification in northern region of India. *Clean Technol. Environ. Policy* **2020**, *22*, 579–590. [CrossRef]
22. Suresh, V.; Muralidhar, M.; Kiranmayi, R. Modelling and optimization of an off-grid hybrid renewable energy system for electrification in a rural areas. *Energy Rep.* **2020**, *6*, 594–604. [CrossRef]
23. Vendoti, S.; Muralidhar, M.; Kiranmayi, R. Techno-economic analysis of off-grid solar/wind/biogas/biomass/fuel cell/battery system for electrification in a cluster of villages by HOMER software. *Environ. Dev. Sustain.* **2020**, *23*, 351–372. [CrossRef]
24. Sharma, H.; Pal, N.; Sadhu, P.K. Modeling and Simulation of Off-Grid Power Generation System Using Photovoltaic. *Int. J. Power Electron. Drive Syst. (IJPEDS)* **2015**, *13*, 418–424. [CrossRef]
25. Lotfi, R.; Kargar, B.; Hoseini, S.H.; Nazari, S.; Safavi, S.; Weber, G.-W. Resilience and sustainable supply chain network design by considering renewable energy. *Int. J. Energy Res.* **2021**, *45*, 17749–17766. [CrossRef]
26. Sambhi, S.; Sambhi, S.; Bhadoria, V.S. IoT based optimized and secured ecosystem for energy internet: The state of the art. In *Internet of Things in Business Transformation: Developing an Engineering and Business Strategy for Industry 5.0*; Scrivener Publishing LLC: Beverly, MA, USA, 2021; pp. 91–126. [CrossRef]
27. Chambon, C.L.; Karia, T.; Sandwell, P.; Hallett, J.P. Techno-economic assessment of biomass gasification-based mini grids for productive energy applications: The case of rural India. *Renew. Energy* **2020**, *154*, 432–444. [CrossRef]

28. Mehregan, M.; Abbasi, M.; Hashemian, S.M. Technical, economic and environmental analyses of combined heat and power (CHP) system with hybrid prime mover and optimization using genetic algorithm. *Sustain. Energy Technol. Assess.* **2022**, *49*, 101697. [[CrossRef](#)]
29. Yadav, D.; Singh, N.; Bhadoria, V.S. Comparison of MPPT Algorithms in Stand-Alone Photovoltaic (PV) System on Resistive Load. In *Machine Intelligence and Smart Systems*; Agrawal, S., Kumar Gupta, K., Chan, J.H., Agrawal, J., Gupta, M., Eds.; Algorithms for Intelligent Systems; Springer: Singapore, 2021. [[CrossRef](#)]
30. Sharma, H.; Pal, N.; Singh, Y.; Sadhu, P.K. Development and Simulation of Stand Alone Photovoltaic Model Using Matlab/Simulink. *Int. J. Power Electron. Drive Syst.* **2015**, *6*, 703. [[CrossRef](#)]
31. Cai, W.; Li, X.; Maleki, A.; Pourfayaz, F.; Rosen, M.A.; Nazari, M.A.; Bui, D.T. Optimal sizing and location based on economic parameters for an off-grid application of a hybrid system with photovoltaic, battery and diesel technology. *Energy* **2020**, *201*, 117480. [[CrossRef](#)]
32. Ndwali, P.K.; Njiri, J.G.; Wanjiru, E.M. Optimal Operation Control of Microgrid Connected Photovoltaic-Diesel Generator Backup System Under Time of Use Tariff. *J. Control Autom. Electr. Syst.* **2020**, *31*, 1001–1014. [[CrossRef](#)]
33. Hoseinzadeh, S.; Garcia, D.A. Techno-economic assessment of hybrid energy flexibility systems for islands' decarbonization: A case study in Italy. *Sustain. Energy Technol. Assess.* **2022**, *51*, 101929. [[CrossRef](#)]
34. Fotis, G.; Dikeakos, C.; Zafeiropoulos, E.; Pappas, S.; Vita, V. Scalability and Replicability for Smart Grid Innovation Projects and the Improvement of Renewable Energy Sources Exploitation: The FLEXITRANSTORE Case. *Energies* **2022**, *15*, 4519. [[CrossRef](#)]
35. Ao, H.X.; Eftekhari, M.; Aungkulanon, P.; Almutairi, K.; Mostafaepour, A. Impact of economic and government investment in residential solar power plant on energy system sustainability. *Sustain. Energy Technol. Assess.* **2022**, *52 Pt A*, 102050. [[CrossRef](#)]
36. Das, U.; Nandi, C.; Bhattacharjee, S.; Mandal, S. Energy Impacts on Climate Change: Issues, Challenges and Solutions with Clean Conversion Technology. In *Climate Change in the Mediterranean and Middle Eastern Region*; Leal Filho, W., Manolas, E., Eds.; Climate Change Management; Springer: Cham, Switzerland, 2022. [[CrossRef](#)]
37. Pravin, P.S.; Luo, Z.; Li, L.; Wang, X. Learning-based scheduling of industrial hybrid renewable energy systems. *Comput. Chem. Eng.* **2022**, *159*, 107665. [[CrossRef](#)]
38. Yadav, R.K.; Bhadoria, V.S.; Hrisheeksha, P.N. Technical and Financial Assessment of a Grid Connected Solar PV Net Metering System for Residential Community. In Proceedings of the 2019 2nd International Conference on Power Energy, Environment and Intelligent Control (PEEIC), Greater Noida, India, 18–19 October 2019; pp. 299–303. [[CrossRef](#)]
39. Zhang, L.; Li, S.; Hu, Y.; Nie, Q. Economic optimization of a bioenergy-based hybrid renewable energy system under carbon policies—From the life-cycle perspective. *Appl. Energy* **2022**, *310*, 118599. [[CrossRef](#)]
40. The Solar Quarterly. Available online: [https://bookstore.teri.res.in/docs/magazines/TSQ_Jan%202011_\(Part2\).pdf](https://bookstore.teri.res.in/docs/magazines/TSQ_Jan%202011_(Part2).pdf) (accessed on 5 August 2020).
41. Ladakh Climate. Available online: <https://www.thethirdpole.net/2018/09/25/climate-ladakh-agriculture> (accessed on 5 August 2020).
42. Sherwani, A.F.; Asjad, M.; Haleem, A. Performance evaluation of solar photovoltaic electricity-generating systems: An Indian perspective. *Int. J. Sustain. Eng.* **2019**, *12*, 70–75. [[CrossRef](#)]
43. Ramesh, M.; Saini, R.P. Dispatch strategies based performance analysis of a hybrid renewable energy system for a remote rural area in India. *J. Clean. Prod.* **2020**, *259*, 120697. [[CrossRef](#)]
44. Ar'evalo, P.; Benavides, D.; Lata-García, J.; Jurado, F. Energy control and size optimization of a hybrid system (photovoltaic-hydrokinetic) using various storage technologies. *Sustain. Cities Soc.* **2020**, *52*, 101773. [[CrossRef](#)]
45. Aziz, A.S.; Tajuddin, M.F.N.; Hussain, M.K.; Adzman, M.R.; Ghazali, N.H.; Ramli, M.A.; Zidane, T.E.K. A new optimization strategy for wind/diesel/battery hybrid energy system. *Energy* **2021**, *239*, 122458. [[CrossRef](#)]
46. Ahamed, A.; Fayaz, R.M.R.; Vibahar, S.; Purusothaman, M.; Gurudevan, P.R. Optimization of Hybrid Microgrid of Renewable Energy Efficiency Using Homer Software. *Rev. Gestão Inovação Tecnol.* **2021**, *11*, 3427–3441. [[CrossRef](#)]
47. Kapoor, S.; Sharma, A.K. Techno-economic analysis by homer-pro approach of solar on-grid system for Fatehpur-Village, India. *J. Phys. Conf. Ser.* **2021**, *2070*, 012146. [[CrossRef](#)]
48. Chaurasia, R.; Gairola, S.; Pal, Y. Technical, economic, and environmental performance comparison analysis of a hybrid renewable energy system based on power dispatch strategies. *Sustain. Energy Technol. Assess.* **2022**, *53 Pt D*, 102787. [[CrossRef](#)]
49. Adewumi, O.B.; Fotis, G.; Vita, V.; Nankoo, D.; Ekonomou, L. The Impact of Distributed Energy Storage on Distribution and Transmission Networks' Power Quality. *Appl. Sci.* **2022**, *12*, 6466. [[CrossRef](#)]
50. Alzahrani, A.M.; Zohdy, M.; Yan, B. An Overview of Optimization Approaches for Operation of Hybrid Distributed Energy Systems with Photovoltaic and Diesel Turbine Generator. *Electr. Power Syst. Res.* **2021**, *191*, 106877. [[CrossRef](#)]
51. Ram, K.; Swain, P.K.; Vallabhaneni, R.; Kumar, A. Critical assessment on application of software for designing hybrid energy systems. *Mater. Today Proc.* **2022**, *49 Pt 2*, 425–432. [[CrossRef](#)]
52. Fathima, A.H.; Palanisamy, K. Optimization in microgrids with hybrid energy systems—A review. *Renew. Sustain. Energy Rev.* **2015**, *45*, 431–446. [[CrossRef](#)]
53. Kumar, P.; Pal, N.; Sharma, H. Optimization and techno-economic analysis of a solar photo-voltaic/biomass/diesel/battery hybrid off-grid power generation system for rural remote electrification in eastern India. *Energy* **2022**, *247*, 123560. [[CrossRef](#)]

54. Zafeiropoulou, M.; Mentis, I.; Sijakovic, N.; Terzic, A.; Fotis, G.; Maris, T.I.; Vita, V.; Zoulias, E.; Ristic, V.; Ekonomou, L. Forecasting Transmission and Distribution System Flexibility Needs for Severe Weather Condition Resilience and Outage Management. *Appl. Sci.* **2022**, *12*, 7334. [CrossRef]
55. Climate Turtuk (India). Available online: <https://en.climate-data.org/asia/india/jammu-and-kashmir/turtuk-565427/> (accessed on 10 August 2021).
56. Razmjoo, A.; Shirmohammadi, R.; Davarpanah, A.; Pourfayaz, F.; Aslani, A. Stand-alone hybrid energy systems for remote area power generation. *Energy Rep.* **2019**, *5*, 231–241. [CrossRef]
57. Sijakovic, N.; Terzic, A.; Fotis, G.; Mentis, I.; Zafeiropoulou, M.; Maris, T.I.; Zoulias, E.; Elias, C.; Ristic, V.; Vita, V. Active System Management Approach for Flexibility Services to the Greek Transmission and Distribution System. *Energies* **2022**, *15*, 6134. [CrossRef]
58. Wang, Y.; Hu, Q.; Li, L.; Foley, A.; Srinivasan, D. Approaches to wind power curve modeling: A review and discussion. *Renew. Sustain. Energy Rev.* **2019**, *116*, 109422. [CrossRef]
59. Homer Pro 3.15. Available online: <https://www.homerenergy.com/products/pro/docs/latest/index.html> (accessed on 14 August 2020).
60. Bruen, T.; Marco, J. Modelling and experimental evaluation of parallel connected lithium ion cells for an electric vehicle battery system. *J. Power Sources* **2016**, *310*, 91–101. [CrossRef]
61. DG Set System. Available online: <https://beeindia.gov.in/sites/default/files/3Ch9.pdf> (accessed on 15 September 2020).
62. Petrol Diesel Price. Available online: <https://www.petroldieselprice.com/petrol-diesel-price-in-Leh> (accessed on 26 November 2021).
63. Bhadoria, V.S.; Pachauri, R.K.; Tiwari, S.; Jaiswal, S.P.; Alhelou, H.H. Investigation of Different BPD Placement Topologies for Shaded Modules in a Series-Parallel Configured PV Array. *IEEE Access* **2020**, *8*, 216911–216921. [CrossRef]
64. Capacity Shortage Constraint. Available online: https://www.homerenergy.com/products/pro/docs/latest/capacity_shortage.html (accessed on 19 November 2022).
65. Niyonteze, J.D.D.; Zou, F.; Asemota, G.N.O.; Bimenyimana, S.; Shyirambere, G. Key technology development needs and applicability analysis of renewable energy hybrid technologies in off-grid areas for the Rwanda power sector. *Heliyon* **2020**, *6*, e03300. [CrossRef]
66. Leithon, J.; Werner, S.; Koivunen, V. Cost-aware renewable energy management: Centralized vs. distributed generation. *Renew. Energy* **2020**, *147*, 1164–1179. [CrossRef]
67. Gebrehiwot, K.; Mondal, A.H.; Ringler, C.; Gebremeskel, A.G. Optimization and cost-benefit assessment of hybrid power systems for off-grid rural electrification in Ethiopia. *Energy* **2019**, *177*, 234–246. [CrossRef]
68. Razmjoo, A.; Kaigutha, L.G.; Rad, M.V.; Marzband, M.; Davarpanah, A.; Denai, M. Technical analysis investigating energy sustainability utilizing reliable renewable energy sources to reduce CO₂ emissions in a high potential area. *Renew. Energy* **2021**, *164*, 46–57. [CrossRef]
69. Li, J.; Liu, P.; Li, Z. Optimal design and techno-economic analysis of a solar-wind-biomass off-grid hybrid power system for remote rural electrification: A case study of west China. *Energy* **2020**, *208*, 118387. [CrossRef]
70. Zhang, G.; Xiao, C.; Razmjoo, N. Optimal Operational Strategy of Hybrid PV/Wind Renewable Energy System Using Homer: A Case Study. *Int. J. Ambient Energy* **2021**, *43*, 3953–3966. [CrossRef]
71. Odou, O.D.T.; Bhandari, R.; Adamou, R. Hybrid off-grid renewable power system for sustainable rural electrification in Benin. *Renew. Energy* **2020**, *145*, 1266–1279. [CrossRef]
72. Babaei, R.; Ting, S.-K.D.; Carriveau, R. Feasibility and optimal sizing analysis of stand-alone hybrid energy systems coupled with various battery technologies: A case study of Pelee Island. *Energy Rep.* **2022**, *8*, 4747–4762. [CrossRef]
73. Das, S.; Ray, A.; De, S. Optimum combination of renewable resources to meet local power demand in distributed generation: A case study for a remote place of India. *Energy* **2020**, *209*, 118473. [CrossRef]
74. Murty, V.V.V.S.N.; Kumar, A. Optimal Energy Management and Techno-economic Analysis in Microgrid with Hybrid Renewable Energy Sources. *J. Mod. Power Syst. Clean Energy* **2020**, *8*, 929–940. [CrossRef]
75. Sambhi, S.; Sharma, H.; Kumar, P.; Fotis, G.; Vita, V.; Ekonomou, L. Techno-Economic Optimization of an Off-Grid Hybrid Power Generation for SRM IST, Delhi-NCR Campus. *Energies* **2022**, *15*, 7880. [CrossRef]